Arg-Leu-Tyr-Glu Suppresses Retinal Endothelial Permeability and Choroidal Neovascularization by Inhibiting the VEGF Receptor 2 Signaling Pathway

Wonjin Park[1], Yi-Yong Baek[1], Joohwan Kim[1], Dong Hyun Jo[2], Seunghwan Choi[1], Jin Hyoung Kim[2], Taesam Kim[1], Suji Kim[1], Minsik Park[1], Ji Yoon Kim[3], Moo-Ho Won[4], Kwon-Soo Ha[1], Jeong Hun Kim[2], Young-Guen Kwon[5] and Young-Myeong Kim[1],*

[1]Department of Molecular and Cellular Biochemistry, School of Medicine, Kangwon National University, Chuncheon 24341,
[2]Fight Against Angiogenesis-Related Blindness (FARB) Laboratory, Clinical Research Institute, Seoul National University Hospital, Seoul 03080,
[3]Department of Anesthesiology and Pain Medicine, Hanyang University Hospital, Seoul 04763,
[4]Department of Neurobiology, School of Medicine, Kangwon National University, Chuncheon 24341,
[5]Department of Biochemistry, College of Life Science and Biotechnology, Yonsei University, Seoul 03722, Republic of Korea

Abstract

Vascular endothelial growth factor (VEGF) plays a pivotal role in pathologic ocular neovascularization and vascular leakage via activation of VEGF receptor 2 (VEGFR2). This study was undertaken to evaluate the therapeutic mechanisms and effects of the tetrapeptide Arg-Leu-Tyr-Glu (RLYE), a VEGFR2 inhibitor, in the development of vascular permeability and choroidal neovascularization (CNV). In cultured human retinal microvascular endothelial cells (HRMECs), treatment with RLYE blocked VEGF-A-induced phosphorylation of VEGFR2, Akt, ERK, and endothelial nitric oxide synthase (eNOS), leading to suppression of VEGF-A-mediated hyper-production of NO. Treatment with RLYE also inhibited VEGF-A-stimulated angiogenic processes (migration, proliferation, and tube formation) and the hyperpermeability of HRMECs, in addition to attenuating VEGF-A-induced angiogenesis and vascular permeability in mice. The anti-vascular permeability activity of RLYE was correlated with enhanced stability and positioning of the junction proteins VE-cadherin, β-catenin, claudin-5, and ZO-1, critical components of the cortical actin ring structure and retinal endothelial barrier, at the boundary between HRMECs stimulated with VEGF-A. Furthermore, intravitreally injected RLYE bound to retinal microvascular endothelium and inhibited laser-induced CNV in mice. These findings suggest that RLYE has potential as a therapeutic drug for the treatment of CNV by preventing VEGFR2-mediated vascular leakage and angiogenesis.

Key Words: VEGF, VEGFR2, Choroidal neovascularization, Macular degeneration, Vascular leakage, Permeability

INTRODUCTION

Age-related macular degeneration (AMD) is the most frequent cause of blindness globally and is common in people over 60 years old (Klein *et al*., 2006). This disease is an acquired degeneration of the central portion of the retina, called the macula, manifested by the progressive loss of central vision through non-neovascular (dry AMD) or neovascular derangement (neovascular or wet AMD). Dry AMD is an early stage of the disease and is generally characterized by asymptomatic deposition of clustered extracellular byproducts of photoreceptor metabolism on the retinal pigment epithelium (RPE), known as drusen. As drusen enlarge, the RPE degenerates to a state of geographic atrophy, resulting in the death of RPE cells and subsequent loss of photoreceptor cells and choriocapillaries. Approximately 10-15% of AMD patients eventually develop the wet form (Klein *et al*., 2007). Wet or exudative AMD is characterized by macular leakage of fluid via abnormal choroidal neovascularization (CNV) that results in retinal distortion, scarring, macular destruction, and decreased vision in AMD patients (Hernández-Zimbrón *et al*., 2018). An excessive amount of vascular endothelial growth

factor (VEGF) triggers the growth and leakage of abnormal blood vessels under the macula, resulting in the irreversible loss of central vision (Ferrara, 2010).

VEGF is known to be a potent angiogenic and vascular permeability factor in the pathogenesis of retinal diseases that exhibit CNV (Miler *et al*., 2013). Although VEGF family proteins activate three types of VEGF receptors (VEGFRs), the VEGF-A/VEGFR2 axis elicits the most potent angiogenic activity and vascular permeability. Consequently, anti-VEGF drugs have shown great promise for the treatment of CNV (Angkawinitwong *et al*., 2017; Neves *et al*., 2017). Indeed, intravitreal injection of the VEGF antagonists ranibizumab (Lucentis) and aflibercept (Eylea) has been widely used to treat AMD (Mitchell *et al*., 2018). The humanized anti-VEGF antibody bevacizumab (Avastin) has also been used clinically for the treatment of angiogenesis-based human diseases, including AMD (Spaide *et al*., 2006). These results suggest that inhibiting the VEGF-A/VEGFR2 signaling axis may be a promising strategy for the treatment of angiogenesis and vascular permeability-associated human diseases.

Numerous chemical inhibitors related to the VEGF-A/VEGFR2 signaling pathway have been developed and used as antiangiogenic therapies (Aziz *et al*., 2016; Cao *et al*., 2016). Our recent study showed that the tetrapeptide Arg-Leu-Tye-Glu (RLYE) effectively inhibited VEGF-A-induced angiogenic activity and vascular permeability by binding to VEGFR2, resulting in the suppression of tumor angiogenesis and progression (Baek *et al*., 2015, 2017). This suggests that RLYE can potentially be used to treat wet AMD via the disruption of pathologic ocular neovascularization.

In this study, we evaluated the inhibitory and therapeutic effects of RLYE on angiogenesis and endothelial permeability in VEGF-A-stimulated retinal endothelial cells and in a mouse model of laser-induced CNV. Our data show that RLYE inhibited VEGF-A-induced angiogenesis and vascular permeability without causing cytotoxicity and inhibited laser-induced CNV in a mouse model, providing evidence that this peptide may be useful for treating wet AMD.

MATERIALS AND METHODS

Materials

Antibodies for p-VEGFR2 (Tyr-1175), p-ERK (Thr-202/Tyr-204), p-Akt (Ser-473), p-FAK (Tyr-397), VEGFR2, ERK, Akt, and FAK were obtained from Cell Signaling Technology (Beverly, MA, USA). Antibodies for p-eNOS (Ser-1177), eNOS, VE-cadherin, and β-catenin were purchased from BD Bioscience (San Diego, CA, USA). Antibodies for ZO-1 and claudin-5 and isolectin B4-647 were purchased from Invitrogen Life Technologies (Carlsbad, CA, USA). VEGF-A, [³H]-thymidine, and [¹⁴C]-sucrose were obtained from R&D Systems (Minneapolis, MN, USA) and Amersham (Aylesbury, UK). Fetal bovine serum (FBS) and N^G-methyl-L-arginine acetate were purchased from MEDIAN Life Science (Houston, TX, USA) and Sigma-Aldrich (St. Louis, MO, USA), respectively. RLYE and fluorescein isothiocyanate (FITC)-conjugated RLYE were purchased from Peptron (Daejeon, Korea).

Cell culture

Human retina microvascular endothelial cells (HRMECs) were purchased from Cell Systems (Kirkland, WA, USA) and grown in complete classic medium (4Z0-500, Cell Systems) at 37°C in a humidified incubator with 5% CO_2. For the experiments, cells were used between passages 3-5.

In vitro angiogenesis assay

Angiogenic activity was determined by measurements of proliferation, migration, and tube formation of cultured HRMECs stimulated with 10 ng/mL VEGF-A following pretreatment with 0.15 nM RLYE for 30 min as described previously (Baek *et al*., 2015, 2017). Endothelial cell proliferation was determined by a [³H]-thymidine incorporation assay. Briefly, HRMECs were cultured at a density of 2×10⁴ cells/well in gelatin-coated 24-well plates overnight and then further cultured for an additional 6 h in M199 medium containing 1% FBS. The cells were pretreated with 0.15 nM RLYE for 30 min and stimulated with 10 ng/mL VEGF-A for 24 h, followed by the addition of 0.5 μCi/mL [³H]-thymidine and incubation for 6 h. [³H]-Thymidine incorporated into high-molecular-weight DNA was determined using a liquid scintillation counter (Perkin Elmer, Gaithersburg, MD, USA) as described previously (Baek *et al*., 2015, 2017). Chemotactic migration and motility of HRMEC were determined using Boyden chambers (24-well Transwell plates, Corning Costar) with 6.5-mm diameter polycarbonate filters (8 μm pore size). Briefly, the lower surface of the filter was coated with 2% gelatin (10 μg). M199 media (1% FBS) containing VEGF-A (10 ng/mL) was placed in the lower chamber. HRMECs (1×10⁶ cells/mL of M199 medium containing 1% FBS) were pre-incubated with 0.15 nM RLYE for 30 min at room temperature. An aliquot (100 μL) from the cell suspensions was loaded into each of the upper wells. After incubation in a CO_2 incubator for 4 h, the cells were fixed and stained with hematoxylin and eosin (H&E). Non-migrating cells on the upper surface of the filter were removed by wiping with a cotton swab and chemotaxis was observed and quantified using a computer-aided inverted phase-contrast microscope. Tube formation was determined after culturing the HRMECs on growth factor-reduced Matrigel (Baek *et al*., 2015, 2017). Twenty-four-well culture plates were coated with 250 μL of growth factor-reduced Matrigel (10 mg/mL). The HRMECs cultured in M199 media containing 1% FBS for 6 h were collected and plated onto the Matrigel layer at a density of 2.5×10⁵ cells/well. The cells were pretreated with RLYE (0.15 nM) for 30 min and stimulated with VEGF-A (10 ng/mL) in a CO_2 incubator for 20 h. Tube-like structure formation was observed using a phase-contrast microscope. The degree of tube formation was quantified by measuring the length of the tubes in randomly chosen low-power fields using ImageJ software (NIH, Bethesda, MA, USA).

Nitric oxide (NO) measurement

Intracellular NO levels were measured using DAF-FM diacetate (Molecular Probes, Eugene, OR, USA) according to the manufacturer's instructions. HRMECs were pretreated with RLYE (0.15 nM) and stimulated with VEGF-A (10 ng/mL) for 15 min. The HRMECs were then incubated with 5 M DAF-FM diacetate for 20 min in a CO_2 incubator, then washed in flash medium, and the fluorescence images were captured from at least 10 randomly selected cells per dish using a confocal laser microscope. The relative levels of intracellular NO were quantified from the DAF-FM fluorescence intensity.

Immunofluorescence staining

HRMECs were grown as a monolayer on 2% gelatin-coated cover glasses and cultured for 6 h in M199 medium containing 1% FBS. The cells were pretreated with 0.15 nM RLYE for 30 min and stimulated with 10 ng/mL VEGF-A for 1 h. The cells were then fixed with 3.7% formaldehyde for 15 min at 4°C, permeabilized with 0.1% Triton X-100 for 30 min at 4°C, and stained for 3 h with antibodies for VE-cadherin (1:50), ZO-1 (1:100), claudin-5 (1:100), and β-catenin (1:100). The cells were then incubated with an Alexa Fluor 555 secondary antibody (1:100, Invitrogen Life Technologies) for 1 h. Nuclei were visualized with 4′,6-diamidino-2-phenylindole (DAPI, Sigma-Aldrich) staining. Fluorescence was observed by confocal laser scanning microscopy (LSM-880, Carl Zeiss, Oberkochen, Germany).

Endothelial cell hyperpermeability assay

To determine [^{14}C]-Sucrose permeability in HRMECs, 24-well Transwell plates with 6.5-mm diameter polycarbonate membrane insert (0.4 μm pore size) were used. HRMECs were incubated with M199 containing 1% FBS for 4 h and treated for 30 min with RLYE (0.15 nM), followed by stimulation with VEGF-A (20 ng/mL) for 1 h. Fifteen microliters of [^{14}C]-sucrose (0.8 μCi/mL) was added to the upper compartment. After incubation for 30 min, the amount of radioactivity that diffused into the lower compartment was measured using a liquid scintillation counter.

Western blot analysis

HRMECs were lysed in RIPA buffer [50 mmol/L Tris-HCl (pH 8.0), 150 mM NaCl, 1% NP-40, 0.5% deoxycholic acid, 0.1% sodium dodecyl sulfate (SDS)]. Cell lysates (50 μg protein) were electrophoresed on SDS-polyacrylamide gel and transferred to polyvinyldifluoride membranes. The membranes were incubated with an antibody against each target protein for 2 h. After three washes, the membranes were incubated with a HRP-conjugated secondary antibody. Protein levels were detected by an enhanced chemiluminescence system

as described previously (Park *et al.*, 2019) and quantified by using ImageJ software (NIH).

Animals

Six-week-old male C57BL/6 mice were purchased from Orient Bio Inc (Sungnam, Korea). The mice were housed in a specific pathogen-free animal facility with a constant temperature of 21 ± 2°C, relative humidity of 45 ± 15%, and a 12 h-light/dark cycle and provided free access to standard food and water. All animal experiments were performed in accordance with the guidelines of the Institutional Animal Care and Use Ethics Committee of Kangwon National University (KW-181109-1). Moreover, this investigation conformed to the Guide for the Care and Use of Laboratory Animals published by the United States National Institutes of Health (NIH Publication, 8th edition, 2011).

Vascular permeability assay

The Miles assay was performed to determine vascular permeability in 6-week-old male C57BL/6 mice. The mice were carefully shaved on both flanks 2 days before the experiment and intraperitoneally injected with RLYE (1 mg/kg, volume 100 μL). After 20 min, the mice were intravenously injected with 1% Evans blue following anesthesia and, 10 min later, intradermally injected with 50 μL of PBS and VEGF-A (100 ng/50 μL). The mice were euthanized after 20 min and the dorsal skin was carefully removed. The lesions were resected using an 8-mm biopsy punch, and Evans blue dye was extracted from the skin with 1 mL of formamide at room temperature for 5 days. The concentration of the Evans blue dye was determined spectrophotometrically at 620 nm.

Matrigel plug assay

Six-week-old male C57BL/6 mice were injected subcutaneously with 0.5 mL of Matrigel containing heparin (30 units), VEGF-A (100 ng), or RLYE (0.75 pmol) after anesthesia with pentobarbital (50 mg/kg, intraperitoneally). The mice were euthanized 7 days later and the Matrigel plugs were retrieved
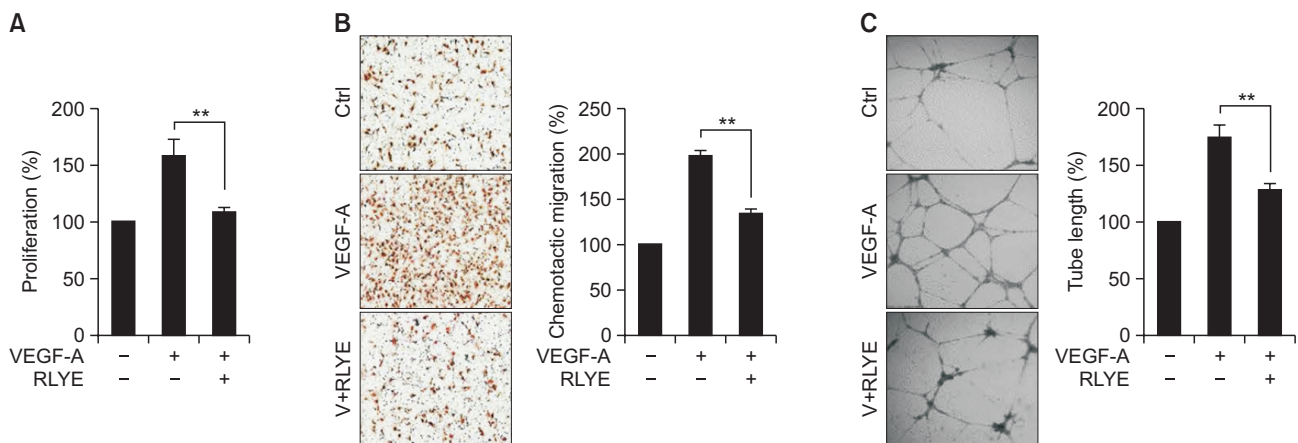
Fig. 1. RLYE decreases VEGF-induced angiogenic activity in HRMECs. HRMECs were pretreated with or without RLYE (0.15 nM) for 30 min prior to stimulation with VEGF-A (10 ng/mL) for the indicated time periods, followed by assessment of angiogenic activity. (A) After 24 h of stimulation, cell proliferation was determined by the [^{3}H]-thymidine incorporation assay (n=4). (B) After 4 h of stimulation, chemotactic cell migration was determined by the Boyden chamber assay. The migrated cells were quantified by counting the cells using a computer-aided optical microscope (n=4). (C) After 20 h of stimulation, tube-like structures were photographed using an inverted phase-contrast microscope, and the tube length was quantified using ImageJ software (NIH) (n=4). **$p<0.01$.

and imaged. The hemoglobin content in the Matrigel plugs was measured using Drabkin's reagent Kit 525 (Sigma-Aldrich) to quantify functional blood vessel formation.

Laser photocoagulation-induced CNV

Laser-induced CNV was performed as described previously (Jo *et al.*, 2017). Male C57BL/6 mice were fully anesthetized with an intraperitoneal injection of ketamine (80 mg/kg)-xylazine (10 mg/kg) and the pupils were dilated with 1% tropicamide (Alcon Laboratories, Fort Worth, TX, USA). Then, the laser was delivered to the retina at the 3, 6, 9, and 12 o'clock positions of 2 disc diameters from the optic disc using an indirect head set delivery system (Iridex, Mountain View, CA, USA) and a custom 810-nm diode laser system (Ilooda, Suwon, Korea). The success of photocoagulation was evaluated by the bubble at the laser site or the popping sound verifying the rupture of Bruch's membrane. Only the successful photocoagulated sites were included in the analysis. Mice were intravitreally injected with 2 μL of RLYE (1.5 nM), EYLR (1.5 nM, as a negative control), or PBS (as a control) 10 days after laser photocoagulation.

Quantitative analysis of CNV

For histological examination, the eyes were enucleated from the sacrificed mice by inhalation of CO_2 gas 14 days after laser photocoagulation and fixed in 3.7% formaldehyde for 24 h at room temperature. After removal of the anterior segments, the posterior eyecups were embedded in paraffin. Sagittal sections of the tissues into 6 μm-thickness were prepared by cutting through the center of the eye at the site of laser

photocoagulation. The sections were stained with H&E and assessed by light microscopy. In addition, fluorescein angiography was also performed on day 14 after laser photocoagulation. The mice were anesthetized with an intraperitoneal injection of ketamine (80 mg/kg)-xylazine (10 mg/kg) and perfused with FITC-dextran (MW, 500 kDa; Sigma-Aldrich) dissolved in PBS. After 1 h of perfusion, the eyes were enucleated from the sacrificed mice by inhalation of CO_2 gas and fixed in 4% paraformaldehyde for 1 h. After removal of the cornea, lens, and vitreous material, the retinas were carefully peeled from the RPE-choroid-scleral complexes. The complexes were mounted on a microscope slide using an aqueous mounting medium (Dako, Agilent Technologies, Santa Clara, CA, USA) and observed under a fluorescence microscope (BX50, Olympus, Tokyo, Japan) at ×400 magnification. The CNV areas were quantified using ImageJ software (NIH).

FITC-RLYE binding assay in the mouse retina

After inhalational anesthesia with isoflurane, six-week-old male C57BL/6 mice were intravitreally injected with 2 μL of PBS, VEGF-A (50 ng/2 μL), or RLYE (1.5 nM) 5 h prior to intravitreal FITC-RLYE (2 μL of 1.5 nM) administration. After 24 h, the mice were anesthetized with an intraperitoneal injection of Avertin (200 mg/250 μL/kg) and perfused (via the left ventricle) with PBS for 7 min (30 mL/min, total 210 mL) and 4% paraformaldehyde (90 mL) for 3 min. The eyes were isolated and fixed with 4% paraformaldehyde for 2 h. Retinas were dissected, immunostained with isolectin B4-647 (1:200), and flat-mounted on glass slides. Fluorescence in the retinas was observed by confocal laser scanning microscopy (LSM-
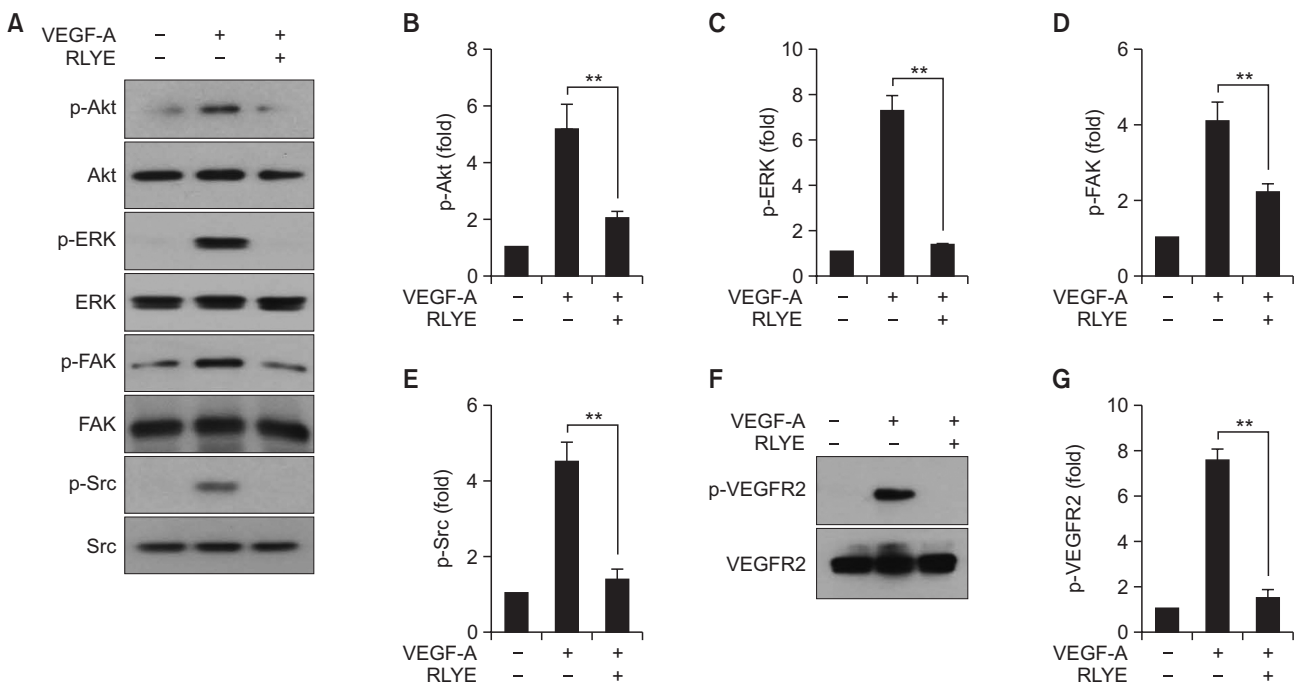
Fig. 2. RLYE blocks VEGF-A-induced angiogenic signaling in HRMECs. HRMECs were pretreated with or without RLYE (0.15 nM) for 30 min and stimulated with VEGF-A (10 ng/mL) for 15 min. (A) Cell lysates were separated by SDS-PAGE, followed by Western blotting to determine the protein and phosphorylation levels of Akt, ERK, FAK, and Src. (B-E) Levels of phosphorylated target genes were defined as a ratio of phosphorylated and non-phosphorylated proteins following protein quantitation using ImageJ software (NIH) (n=3). (F, G) Level of VEGFR2 phosphorylation was determined in cell lysates by Western blotting and quantified using ImageJ software (NIH) (n=3). **$p<0.01$.

880, Carl Zeiss). FITC-RLYE binding in retinal vessels was quantitatively analyzed by measuring the intensities of whole retina tissues.

Statistical analysis

Quantitative data are expressed as the means ± SEM of at least three separate experiments performed in triplicate. Statistical analysis was performed using GraphPad Prism 6 software (GraphPad, Inc., La Jolla, CA, USA). Statistical significance was determined using either one-way ANOVA or the Student's *t*-test, depending on the experimental group analyzed. Significance was established at a *p*-value<0.05.

RESULTS

### RLYE suppresses VEGF-induced angiogenesis in HRMECs

Endothelial cells are highly specialized in organ-specific functions and responses to environmental cues (Aird, 2006; Liu *et al*., 2008; Langenkamp and Molema, 2009). Therefore,

we examined whether RLYE inhibits VEGF-A-induced angiogenesis in cultured HRMECs, although in our previous studies RLYE was shown to exhibit an anti-angiogenic effect in human umbilical vein endothelial cells (HUVECs) (Baek *et al*., 2015, 2017). Treating HRMECs with RLYE significantly inhibited VEGF-A-induced proliferation, a typical characteristic of angiogenesis, as determined by the [³H]-thymidine incorporation assay (Fig. 1A). Treatment with RLYE also markedly inhibited VEGF-A-induced migration and tube formation in HRMECs (Fig. 1B, 1C). These results suggest that RLYE inhibits VEGF-A-mediated angiogenic activity not only in HRMECs, but also in HUVECs.

RLYE blocks angiogenic signaling in VEGF-A-stimulated HRMECs

VEGF-A promotes angiogenesis mostly through the activation of VEGFR2 and its downstream signaling cascades (Taimeh *et al*., 2013), and RLYE has been shown to bind to VEGFR2, interfering with the interaction between VEGF-A and VEGFR2 in HUVECs (Baek *et al*., 2017). Therefore, we
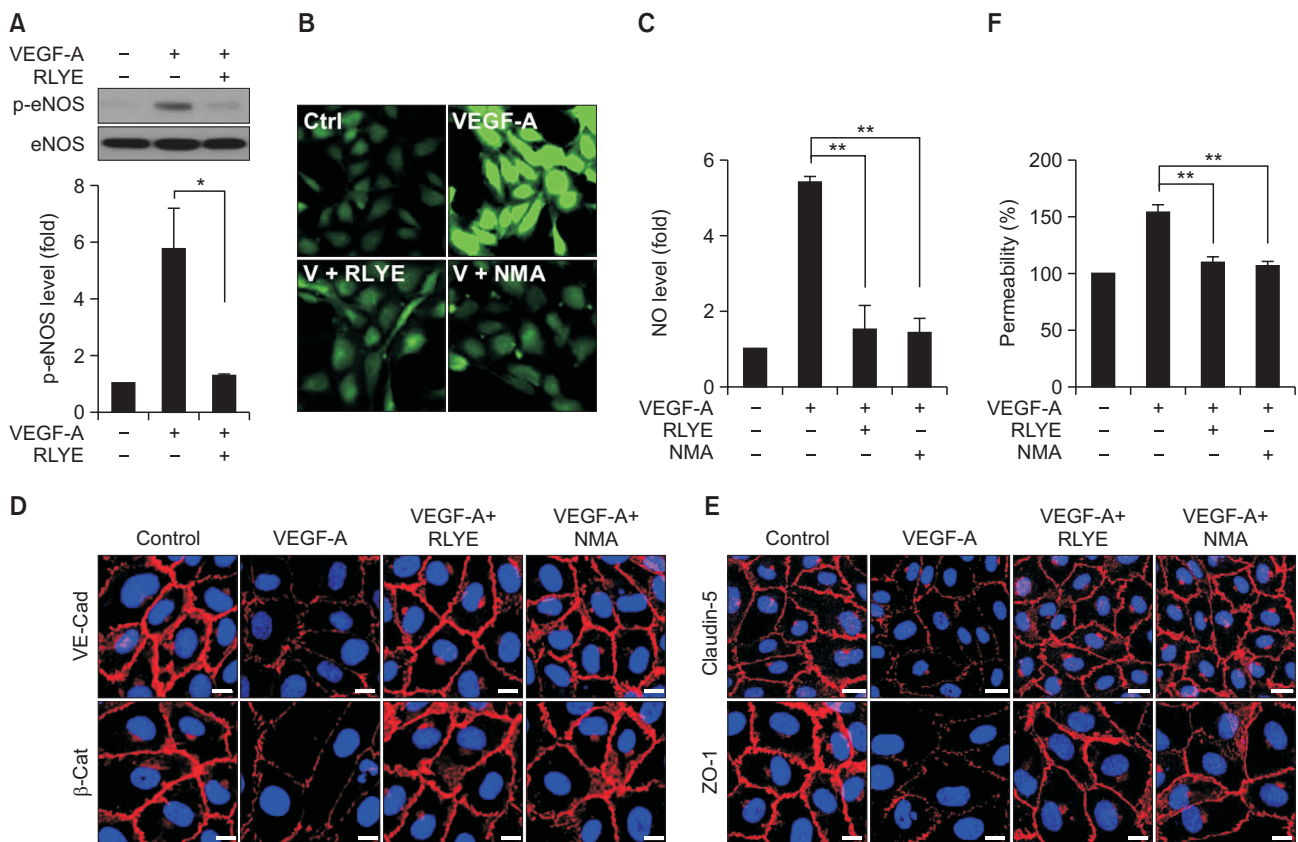
Fig. 3. RLYE inhibits the VEGF-A-induced eNOS/NO pathway, endothelial cell junction breakage, and hyperpermeability in HRMECs. (A) HRMECs were pretreated with RLYE (0.15 nM) for 30 min and stimulated with VEGF (10 ng/mL) for 15 min. Levels of phosphorylated eNOS was determined in cell lysates by western blotting and quantified using ImageJ software (NIH) (n=3). (B, C) HRMECs were pretreated with RLYE (0.15 nM) and NMA (1 mM) for 30 min and stimulated with VEGF (10 ng/mL) for 15 min. Levels of intracellular NO production were measured by confocal microscopy using DAF-FM and quantified using ImageJ software (NIH) (n=6). (D, E) HRMECs grown in monolayers were pretreated with RLYE (0.15 nM) and NMA (1 mM) for 30 min and stimulated with VEGF (10 ng/mL) for 1 h. VE-cadherin, β-catenin, claudin-5, and ZO-1 were immunostained with their specific antibodies and secondary antibodies conjugated to Alexa Fluor 555. Images were obtained with a confocal microscope. Scale bar=10 μm. (F) HRMECs grown in the upper chambers of Transwell plates were pretreated with or without RLYE (0.15 nM) and NMA (1 mM) for 30 min and stimulated with 20 ng/mL of VEGF. Endothelial cell hyperpermeability was determined by measuring the amount of [¹⁴C]-sucrose that diffused through the endothelial cell monolayers (n=3). *p<0.05, **p<0.01.

further examined whether RLYE could inhibit the VEGF-A-induced signaling pathways in HRMECs. Treatment of HRMECs with RLYE inhibited the VEGF-A-induced phosphorylation of Akt, ERK, Src, and FAK (Fig. 2A), molecules known to be crucial mediators of endothelial cell functions during angiogenesis, such as survival, proliferation, and migration (Hofer and Schweighofer, 2007). In addition, RLYE treatment resulted in statistically significant inhibition of the multiple signaling pathways activated by VEGF-A (Fig. 2B-2E). Moreover, the peptide effectively blocked the increased phosphorylation of the apical signal mediator VEGFR2 at Tyr 1175 in HRMECs stimulated with VEGF-A (Fig. 2F, 2G). These results indicate that RLYE potently blocked VEGF-A-induced retinal angiogenesis by inhibiting VEGFR2 activation and its downstream signaling cascade in HRMECs.

RLYE inhibits the VEGF-A-induced eNOS/NO signaling axis and endothelial hyperpermeability in HRMECs

Since Akt-dependent endothelial nitric oxide synthase (eNOS) activation stimulates NO production, which plays an important role in angiogenesis and vascular permeability (Karar and Maity, 2011; Shi *et al.*, 2012; Di Lorenzo *et al.*, 2013), we examined the inhibitory effect of RLYE on the eNOS/NO pathway. As expected, VEGF-A stimulated the phosphorylation of eNOS at Ser1177 in HRMECs, but this phosphorylation was reduced by co-treatment with RLYE to almost the basal levels observed in the unstimulated control cells (Fig. 3A). As a result, RLYE markedly inhibited the VEGF-A-mediated increase in NO production in HRMECs, with an inhibitory effect comparable to that of the NOS inhibitor NMA (Fig. 3B, 3C). Because NO is essential for the increased retinal endothelial barrier permeability induced by VEGF-A (Di Lorenzo *et al.*, 2013), we examine the effect of RLYE on endothelial junctions and permeability in an *in vitro* blood-retinal barrier (BRB) model using cultured HRMECs stimulated with VEGF-A. Treatment with RLYE or NMA significantly rescued the VEGF-A-mediated loss of the adherence junction protein VE-cadherin and its binding partner β-catenin at the cell-cell boundary of HRMECs (Fig. 3D, Supplementary Fig. 1A, 1B). In addition, RLYE and NMA also inhibited the VEGF-A-induced loss of the tight junction components claudin-5 and ZO-1 from the cell-cell contact sites of HRMECs (Fig. 3E, Supplementary Fig. 1C, 1D). As a result, RLYE and NMA significantly attenuated endothelial hyperpermeability in HRMECs stimulated with VEGF-A as determined by the [^{14}C]-sucrose leakage assay (Fig. 3F). Collectively, these results suggest that RLYE effectively suppressed the VEGF-A-induced increase in retinal endothelial barrier permeability by inhibiting the VEGFR2-mediated eNOS/NO pathway.

RLYE inhibits VEGF-A-induced neovascularization and vascular permeability in mice

To further confirm the *in vitro* data, we examined the effect of RLYE treatment on VEGF-A-induced neovascularization and vascular permeability in mice using the Matrigel plug assay and the Evans blue-based Miles assay, respectively. Matrigel plugs containing VEGF-A, implanted subcutaneously in mice, showed a dark-red color indicative of neovascularization, whereas the control Matrigel plugs were colorless; however, the plug containing VEGF-A with RLYE was pale or reddish (Fig. 4A), indicating that RLYE inhibited the VEGF-A-induced formation of a functional vasculature. This was further
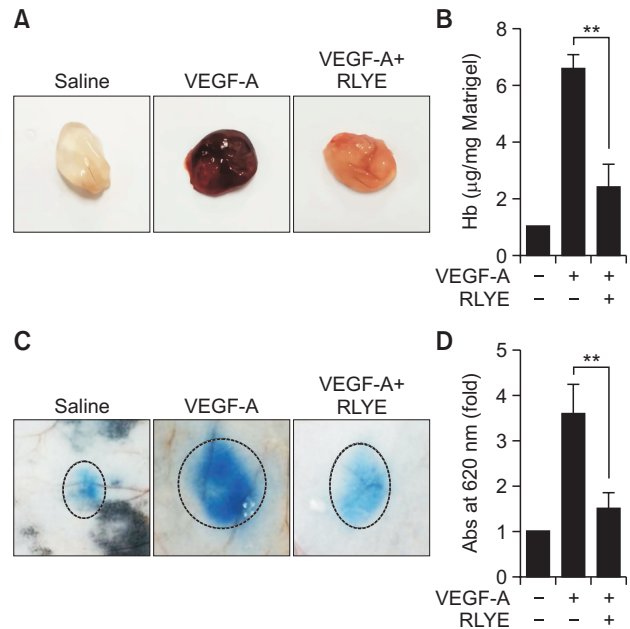

Fig. 4. RLYE inhibits VEGF-A-induced neovascularization and vascular permeability in mice. (A, B) Mice were subcutaneously injected with 0.5 mL of Matrigel containing VEGF-A (100 ng) alone or in combination with RLYE (0.75 pmol). (A) After 7 days, Matrigel plugs were excised from the mice after sacrifice by cervical dislocation and photographed. (B) Hemoglobin (Hb) concentrations were measured after extraction from the Matrigel plugs using the Drabkin method (n=4). (C, D) Mice were injected intraperitoneally with RLYE (1 mg/100 μL/kg). After 4 h, the mice were injected intravenously with 1% Evans blue following anesthesia, followed by intradermal injection of PBS (50 μL/site) or VEGF-A (100 ng/50 μL/site). (C) The mice were euthanized after 20 min, and the dorsal skin was carefully removed and photographed. (D) Evans blue dye was extracted from the skin with formamide, and the dye concentration was determined by spectrophotometry (n=4). **$p<0.01$.

confirmed by measuring the hemoglobin content in the Matrigel (Fig. 4B). Intradermal injection of VEGF-A significantly increased the extravasation of intravascular Evans blue via elevated microvascular leakage in mice, and this increase was markedly suppressed by pretreatment with RLYE (Fig. 4C, 4D). These results suggest that RLYE blocks VEGF-A-induced angiogenesis and vascular permeability in mice.

RLYE binds to retinal vascular endothelial cells in mice

Since RLYE has been shown to bind to VEGFR2 in HUVECs, we next examined whether the peptide would bind to endothelium in retinal vessels after intravitreal injection of FITC-conjugated RLYE in mice. The results showed a significant increase in the binding of RLYE to retinal microvascular endothelium, as determined by the confirmation of its co-localization in isolectin B4-stained endothelial cells, and its binding potential was comparatively inhibited by pretreatment with either VEGF-A or the non-fluorescent peptide (Fig. 5A, 5B). However, FITC and FITC-EYLR did not bound to retinal endothelial cells (Supplementary Fig. 2A, 2B). These findings suggest that RLYE competes with VEGF-A in binding to retinal microvascular endothelial cells.
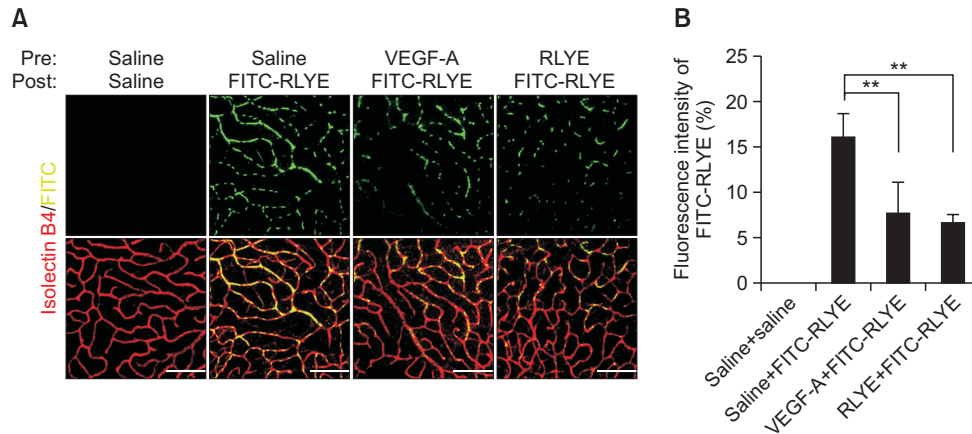
Fig. 5. RLYE binds to retinal microvascular endothelial cells in mice. (A) Mice were intravitreally injected with 2 μL of saline, VEGF-A (50 ng/2 μL), or RLYE (1.5 nM) 5 h prior to intravitreal administration of FITC-RLYE (2 μL of 1.5 nM). After 24 h, the mice were anesthetized and perfused with 4% paraformaldehyde. The retinas were isolated, flat-mounted, and stained with isolectin B4-647. The fluorescence of isolectin B4 and FITC-RLYE was determined by confocal microscopy. (B) The binding activity of RLYE to endothelium was quantified by measuring the fluorescence intensity of FITC-RLYE using ImageJ software (NIH) (n=5). Scale bar=100 μm. **$p<0.01$.

RLYE inhibits laser-induced CNV

The mouse laser-induced CNV model has been used extensively as a crucial mainstay model for studies of neovascular AMD (Shah *et al.*, 2015). By administering targeted laser injury to the RPE and Bruch's membrane, the procedure induces angiogenesis, mitogenesis, and vascular permeability, which are the pathogenic hallmarks of neovascular AMD (Lambert *et al.*, 2013). To verify the biological activity of RLYE in negatively regulating laser-induced CNV in mice, the peptide was injected into the vitreous cavity of mice after laser photocoagulation. Histopathological examination using H&E staining showed that RLYE treatment significantly decreased laser-induced CNV areas in the retina compared to mice administrated PBS, whereas the control peptide (EYLR) that does not exhibit antiangiogenic activity did not significantly affect laser-induced CNV lesions (Fig. 6A, 6B). Moreover, fluorescein angiography using FITC-dextran further confirmed that RLYE inhibited the formation of laser-induced CNV compared to either PBS or EYLR injection (Fig. 6C, 6D). These results suggest that RLYE inhibits pathological CNV.

DISCUSSION

VEGF is a potent angiogenic and vascular permeability factor that plays a pivotal role not only in the physiology of embryonic vascular development and wound healing but also in the pathogenesis of many human diseases, including cancer, diabetic retinopathy, and wet AMD (Ferrara *et al.*, 2003; Carmeliet, 2005; Ferrara *et al.*, 2007; Simo and Hernandez, 2008). The VEGF family consists of five VEGF isoforms, namely VEGF-A, -B, -C, -D, and placental growth factor. Among them, VEGF-A is the most abundant and most biologically active form (Ferrara, 2004), and binds both VEGFR1 and VEGFR2 both of which are mainly expressed in endothelial cells. Both receptors are primarily associated with angiogenesis, but also have additional unique biological functions. For example, the binding affinity of VEGFR1 for VEGF-A is one order of magnitude higher than that of VEGFR2, whereas the kinase activity
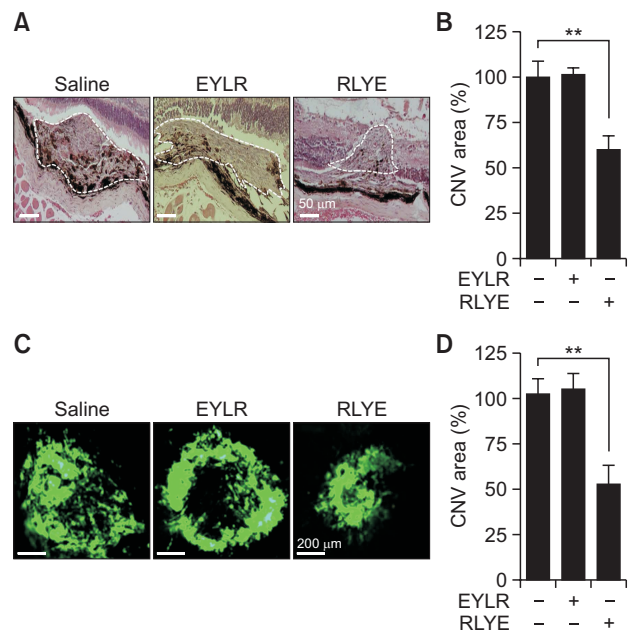
Fig. 6. RLYE inhibits laser-induced CNV. Mice were intravitreally injected with saline, EYLR, or RLYE 10 days after laser photocoagulation. (A, B) The eyes were enucleated from the mice sacrificed by inhalation of CO_2 gas and fixed in 3.7% formaldehyde. Tissue sections were stained with H&E. The CNV areas were quantified using ImageJ software (NIH) (n=6). Scale bar=50 μm. (C, D) Mice were perfused with FITC-dextran dissolved in saline 14 days after laser photocoagulation and observed under a fluorescence microscope. Scale bar=200 μm. The CNV areas were quantified using ImageJ software (NIH) (n=6). **$p<0.01$.

of VEGFR1 is approximately 10-fold weaker than that of VEGFR2 (Shibuya, 2006), indicating that VEGFR2 is the major inducer of angiogenesis under physiological and pathological conditions. Based on this evidence, effective inhibition of the VEGF-A/VEGFR2 pathway serves as a therapeutic strategy

for treating angiogenesis-associated diseases, including wet AMD (Ferrara et al., 2007).

Retinal and choroidal neovascularization are the main causes of visual impairment in several ocular diseases, including wet AMD and diabetic retinopathy. Several factors, like inflammatory and angiogenic factors, are known to be involved in the pathological alteration of retinal and choroidal vessels (Ferrara et al., 2007; Kauppinen et al., 2016); they include VEGF-A, which is mainly associated with the induction of neovascularization and vascular leakage in the retinal and choroidal vessels. Indeed, the expression levels of VEGF-A are also increased in mouse and non-human primate models of retinal neovascularization and are highly correlated with the degree of retinal angiogenesis (Miller et al., 1994; Pierce et al., 1995). Intravitreal administration of VEGF-A-neutralizing chimeric proteins significantly suppressed retinal neovascularization in a murine model of ischemic retinopathy (Aiello et al., 1995). Furthermore, the expression of VEGF-A is known to be elevated in patients with AMD (Grisanti and Tatar, 2008), and patients with pathologic retinal neovascularization have higher levels of VEGF-A expression in ocular tissue than patients without neovascularization (Aiello et al., 1994). Consequently, treatment with anti-angiogenic drugs that inhibit the VEGF-A/VEGFR2 axis is currently still the most potent therapeutic strategy for treating wet AMD, despite the advent of anti-inflammatory therapy as a new treatment option (Holz et al., 2014).

AMD is the leading cause of central visual loss worldwide among patients over 60 years of age. Dry AMD is the most common type, accounting for approximately 90% of all cases and there is currently no treatment available for patients with the dry form, although numerous therapeutic approaches for the treatment of dry AMD are under development. A recent study showed that visual function improved in patients with dry ADM following implantation of a thin synthetic substrate coated with a layer of human embryonic stem cell-derived RPE cells in the retina (Kashani et al., 2018). Moreover, treatment of neovascular or wet AMD has been revolutionized by the availability of intravitreal anti-VEGF agents like bevacizumab and aflibercept (CATT Research Group et al., 2011; Semeraro et al., 2013). These agents effectively inhibit ocular neovascularization triggered by VEGF, and their therapeutic efficacy has been demonstrated to be superior to previous treatment modalities, such as verteporfin photodynamic therapy (Campochiaro et al., 2016). Although anti-VEGF therapy has proven to be useful and promises to improve the vision of patients with wet AMD, the efficacy of anti-VEGF treatments is poor in a subgroup of patients due to VEGF-A gene polymorphism (Park et al., 2014; Veloso et al., 2014). This suggests that individualized therapeutic approaches based on genetic background may be required to generate optimal efficacy in neovascular AMD. To date, many endogenous and synthetic inhibitors of angiogenesis including antibodies, siRNAs, peptides, metabolites, and enzyme inhibitors, have been identified and proposed as potential therapeutic alternatives to target neovascularization and vascular leakage in neovascular AMD (Jo et al., 2017; Bee et al., 2018; Yan et al., 2018). Our data showed that the anti-angiogenic peptide RLYE suppressed laser-induced CNV in mice by blocking VEGF-A-triggered angiogenic signaling, such as Akt, ERK, and FAK, suggesting that this peptide has promising therapeutic applications for the treatment of neovascular AMD.

In addition to the anti-VEGF drugs bevacizumab, aflibercept, and ranibizumab, the anti-VEGFR2 antibody ramucirumab (Cyramza) that selectively binds to s specific epitope on the extracellular domain of VEGFR2 was shown to have similar antiangiogenic activity in cancer treatment to that seen with bevacizumab (Arrieta et al., 2017); this antibody may also elicit therapeutic benefits in patients with wet AMD (Clinical trials.gov identifier NCT01940900). Another anti-VEGFR2 antibody, tanibirumab, has been shown to suppress and regress laser-induced choroidal neovascularization in a rat model (Kim et al., 2014). This evidence suggests that targeted inhibition of VEGFR2 is a useful strategy for treating neovascular AMD and angiogenesis-related disorders. Therefore, numerous small molecule kinase inhibitors (e.g., sunitinib, sorafenib, and axitinib) have been developed to inhibit neovascularization by blocking VEGFR-mediated signaling (Ferrara and Adamis, 2016). Our previous studies demonstrated that RLYE binds specifically to VEGFR2 at the VEGF-A binding site, thereby blocking VEGF-A/VEGFR2 interaction and tumor angiogenesis (Baek et al., 2015, 2017).

Notably, our fluorescence analysis demonstrated that intravitreally administered FITC-RLYE bound directly to the retinal microvascular endothelium in mice in a competitive manner with pretreated VEGF-A or non-conjugated RLYE. This suggests that RLYE binds directly to retinal microvascular endothelial cells by interacting with VEGFR2 in the eye and inhibits VEGF-A-induced angiogenic signaling and retinal neovascularization. We also showed that RLYE treatment inhibited VEGF-A-induced angiogenesis and hyperpermeability in cultured HRMECs and blocked retinal neovascularization in a mouse model of laser-induced CNV. Therefore, RLYE may be a feasible treatment for the improvement of visual acuity by inhibiting CNV associated with neovascular or wet AMD.

Neovascular AMD is characterized by VEGF-A-induced retinal angiogenesis and vascular permeability. Similar to the blood-brain barrier, the BRB is a restrictive physiological barrier that regulates nutrient, ion, protein, and water flux in and out of the retina. VEGF stimulates BRB breakdown and vascular leakage that are implicated in the pathogenesis of ocular diseases, such as neovascular AMD and diabetic retinopathy (Cunha-Vaz et al., 2011). This pathological process is likely to be associated with eNOS-derived NO production, which also contributes to the stimulation of neovascularization. Thus, anti-VEGF strategies are effective in treating BRB breakdown and angiogenesis, which are associated with pathological changes in retinal diseases. We found that RLYE could inhibit VEGF-A-induced breakdown of the BRB, as assessed by the loss of junctional proteins like VE-cadherin and claudin-5 at the cell-cell boundaries of HRMECs, consequently resulting in attenuation of endothelial and vascular hyperpermeability. In addition, RLYE suppressed the VEGF-A-mediated increase in eNOS-derived NO production by inhibiting Akt-mediated eNOS activation, a key signaling pathway downstream of VEGFR2. This suggests that RLYE mitigates microvascular permeability and leakage in the retina by suppressing the eNOS/NO pathway under the pathogenic conditions of neovascular AMD. Collectively, these findings indicate that RLYE can prevent retinal microvascular dysfunction mainly by interfering with the interaction between VEGF-A and VEGFR2 in the retinal microvasculature.

In conclusion, the present study showed that RLYE blocked VEGF-A-induced angiogenesis and vascular leakage in HR-

MECs by interfering with the interaction between VEGF-A and VEGFR2 and inhibited retinal neovascularization in a mouse model of laser-induced CNV. Therefore, RLYE has potential as a therapeutic agent for the treatment of neovascular AMD.

CONFLICT OF INTEREST

The authors have no conflict of interest to declare.

ACKNOWLEDGMENTS

REFERENCES

Aiello, L. P., Avery, R. L., Arrigg, P. G., Keyt, B. A., Jampel, H. D., Shah, S. T., Pasquale, L. R., Thieme, H., Iwamoto, M. A., Park, J. E., Nguyen, H. V., Aiello, L. M., Ferrara, N. and King, G. L. (1994) Vascular endothelial growth factor in ocular fluid of patients with diabetic retinopathy and other retinal disorders. *N. Engl. J. Med.* **331**, 1480-1487.

Aiello, L. P., Pierce, E. A., Foley, E. D., Takagi, H., Chen, H., Riddle, L., Ferrara, N., King, G. L. and Smith, L. E. (1995) Suppression of retinal neovacscularization *in vivo* by inhibition of vascular endothelial growth factor (VEGF) using soluble VEGF-receptor chimeric proteins. *Proc. Natl. Acad. Sci. U.S.A.* **92**, 10457-10461.

Aird, W. C. (2006) Mechanisms of endothelial cell heterogeneity in health and disease. *Circ. Res.* **98**,159-162.

Angkawinitwong, U., Awwad, S., Khaw, P. T., Brocchini, S. and Williams, G. R. (2017) Electrospun formulations of bevacizumab for sustained release in the eye. *Acta Biomater.* **64**,126-136.

Arrieta, O., Zatarain-Barron, Z. L., Cardona, A. F., Carmona, A. and Lopez-Mejia, M. (2017) Ramucirumab in the treatment of non-small cell lung cancer. *Expert. Opin. Drug. Saf.* **5**, 637-644.

Aziz, M. A., Serya, R. A., Lasheen, D. S., Abdel-Aziz, A. K., Esmat, A., Mansour, A. M., Singab, A. N. and Abouzid, K. A. (2016) Discovery of potent VEGFR-2 inhibitors based on Furopyrimidine and thieno-pyrimidine scaffolds as cancer targeting agents. *Sci. Rep.* **6**, 24460.

Baek, Y. Y., Lee, D. K., Kim, J., Kim, J. H., Park, W., Kim, T., Han, S., Jeoung, D., You, J. C., Lee, H., Won, M. H., Ha, K. S., Kwon, Y. G. and Kim, Y. M. (2017) Arg-Ley-Tyr-Glu tetrapeptide inhibits tumor progression by suppressing angiogenesis and vascular permeability via VEGF receptor-2 antagonism. *Oncotarget.* **14**, 11763-11777.

Baek, Y. Y., Lee, D. K., So, J. H., Kim, C. H., Jeoung, D., Lee, H., Choe, J., Won, M. H., Ha, K. S., Kwon, Y. G. and Kim, Y. M. (2015) The tetrapeptide Arg-Leu-Tyr-Glu inhibits VEGF-induced angiogenesis. *Biochem. Biophys. Res. Commun.* **463**, 532-537.

Bee, Y. S., Ma, Y. L., Chen, J., Tsai, P. J., Sheu, S. J., Lin, H. C., Huang, H., Liu, G. S. and Tai, M. H. (2018) Inhibition of experimental choroidal neovascularization by a novel peptide derived from calreticulin anti-angiogenic domain. *Int. J. Mol. Sci.* **19**, 10.

Campochiaro, P. A., Aiello, L. P. and Rosenfeld, P. J. (2016) Anti-vascular endothelial growth factor agents in the treatment of retinal disease: from bench to bedside. *Ophthalmology* **123**, S78-S88.

Cao, L., Weetall, M., Bombard, J., Qi, H., Arasu, T., Lennox, W., Hedrick, J., Sheedy, J., Risher, N., Brooks, P. C., Trifillis, P., Trotta, C., Moon, Y. C., Babiak, J., Almstead, N. G., Colacino, J. M., Davis, T. W. and Peltz, S. W. (2016) Discovery of novel small molecule inhibitors of VEGF expression in tumor cells using a cell-based high throughput screening platform. *PLoS ONE* **11**, e0168366.

Carmeliet, P. (2005) VEGF as a key mediator of angiogenesis in cancer. *Oncology* **69 Suppl 3**, 4-10.

CATT Research Group, Martin, D. F., Maguire, M. G., Ying, G. S., Grunwald, J. E., Fine, S. L. and Jaffe, G. J. (2011) Ranibizumab and bevacizumab for neovascular age-related macular degeneration. *N. Engl. J. Med.* **364**, 1897-1908.

Cunha-Vaz, J., Bernardes, R. and Lobo, C. (2011) Blood-retinal barrier. *Eur. J. Ophthalmol.* **21 Suppl 6**, S3-S9.

Di Lorenzo, A., Lin, M. I., Murata, T., Landskroner-Eiger, S., Schleicher, M., Kothiya, M., Iwakiri, Y., Yu, J., Huang, P. L. and Sessa, W. C. (2013) eNOS-derived nitric oxide regulates endothelial barrier function through VE-cadherin and Rho GTPases. *J. Cell Sci.* **126**, 5541-5552.

Ferrara, N. and Adamis, A. P. (2016) Ten years of anti-vascular endothelial growth factor therapy. *Nat. Rev. Drug. Discov.* **6**, 385-403.

Ferrara, N., Gerber, H. P. and LeCounter, J. (2003) The biology of VEGF and its receptors. *Nat. Med.* **6**, 669-676.

Ferrara, N., Mass, R. D., Campa, C. and Kim, R. (2007) Targeting VEGF-A to treat cancer and age-related macular degeneration. *Annu. Rev. Med.* **58**, 491-504.

Ferrara, N. (2004) Vascular endothelial growth factor: basic science and clinical progress. *Endocr. Rev.* **4**, 581-611.

Ferrara, N. (2010) Vascular endothelial growth factor and age-related macular degeneration: from basic science to therapy. *Nat. Med.* **16**, 1107-1111.

Grisanti, S. and Tatar, O. (2008) The role of vascular endothelial growth factor and other endogenous interplayers in age-related macular degeneration. *Prog. Retin. Eye. Res.* **24**, 372-390.

Hernández-Zimbrón, L. F., Zamora-Alvarado, R., Ochoa-De, la. Paz. L., Velez-Montoya, R., Zenteno, E., Gulias-Cañizo, R., Quiroz-Mercado, H. and Gonzalez-Salinas, R. (2018) Age-related macular degeneration: New paradigms for treatment and management of AMD. *Oxid. Med. Cell. Longev.* **1**, 8374647.

Hofer, E. and Schweighofer, B. (2007) Signal transduction induced in endothelial cells by growth factor receptors involved in angiogenesis. *Thromb. Haemost.* **97**, 355-363.

Holz, F. G., Schmitz-Valckenberg, S. and Fleckenstein, M. (2014) Recent developments in the treatment of age-related macular degeneration. *J. Clin. Invest.* **124**, 1430-1438.

Jo, D. H., Kim, J. H., Yang, W., Kim, H., Chang, S., Kim, D., Chang, M., Lee, K., Chung, J. and Kim, J. H. (2017) Anti-complement component 5 antibody targeting MG4 domain inhibits choroidal neovascularization. *Oncotarget* **8**, 45506-45516.

Karar, J. and Maity, A. (2011) PI3K/Akt/mTOR pathway in angiogenesis. *Front. Mol. NeuroSci.* **4**, 51.

Kashani, A. H., Lebkowski, J. S., Rahhal, F. M., Avery, R. L., Salehi-Had, H., Dang, W., Lin, C. M., Mitra, D., Zhu, D., Thomas, B. B., Hikita, S. T., Pennington, B. O., Johnson, L. V., Clegg, D. O., Hinton, D. R. and Humayun, M. S. (2018) A bioengineered retinal pigment epithelial monolayer for advanced, dry age-related macular degeneration. *Sci. Transl. Med.* **10**, 435.

Kauppinen, A., Jussi, J., Paterno., Blasiak, J., Salminen, A. and Kaarniranta, K. (2016) Inflammation and its role in age-related macular degeneration. *Cell. Mol. Life. Sci.* **73**, 1765-1786.

Kim, J., Kim, T. E., Kim, J. A., Yun, J. H., Sohn, S., Shim, S. R., Lee, S. H. and Kim, S. J. (2014) Intravitreal tanibirumab, a fully human monoclonal antibody against vascular endothelial growth factor receptor 2, partially suppresses and regresses laser-induced choroidal neovascularization in a rat model. *J. Ocul. Pharmacol. Ther.* **10**, 847-853.

Klein, R., Klein, B. E., Knudtson, M. D., Wong, T. Y., Cotch, M. F., Liu, K., Burke, G., Saad, M. F. and Jacobs, D. R., Jr. (2006) Prevalence of age-related macular degeneration in 4 racial/ethnic groups in the multi-ethnic study of atherosclerosis. *Ophthlamology* **113**, 373-380.

Klein, R., Klein, B. E., Knudtson, M. D., Meuer, S. M., Swift, M. and Gangnon, R. E. (2007) Fifteen-year cumulative incidence of age-related macular degeneration: the beaver dam eye study. *Ophthalmology* **114**, 253-262.

Lambert, V., Lecomte, J., Hansen, S., Blacher, S., Conzalez, M. L., Struman, I., Sounni, N. E., Rozet, E., de, Tullio, P., Foidart, J. M., Rakic, J. M. and Noel, A. (2013) Laser-induced choroidal neovascularization model to study age-related macular degeneration in

mice. *Nat. Protoc.* **11**, 2197-2211.

Langenkamp, E. and Molema, G. (2009) Microvascular endothelial cell heterogeneity: general concepts and pharmacological consequences for anti-angiogenic therapy of cancer. *Cell. Tissue. Res.* **335**, 205-222.

Liu, M., Kluger, M. S., D'Alessio, A., García-Cardeña, G. and Pober, J. S. (2008) Regulation of arterial-venous differences in tumor necrosis factor responsiveness of endothelial cells by anatomic context. *Am. J. Pathol.* **72**, 1088-1099.

Miler, J. W., Le, Couter, J., Strauss, E. C. and Ferrara, N. (2013) Vascular endothelial growth factor a in intraocular vascular disease. *Ophthalmology* **120**, 106-114.

Miller, J. W., Adamis, A. P., Shima, D. T., D'Amore, P. A., Moulton, R. S., O'Reilly, M. S., Folkman, J., Dvorak, H. F., Brown, L. F., Berse, B., Yeo, T.-K. and Yeo, K.-T. (1994) Vascular endothelial growth factor/vascular permeability factor is temporally and spatially correlated with ocular angiogenesis in a primate model. *Am. J. Pathol.* **145**, 574-584.

Mitchell, P., Liew, G., Gopinath, B. and Wong, T. Y. (2018) Age-related macular degeneration. *Lancet* **392**, 1147-1159.

Neves, Cardoso, P., Pinheiro, A. F., Meira, J., Pedrosa, A. C., Falcão, M. S., Pinheiro-Costa,J., Falcão-Reis, F. and Carneiro, Â. M. (2017) Switch to aflibercept in the treatment of neovascular AMD: long-term results. *J. Ophthalmol.* **2017**, 6835782.

Park, M., Choi, S., Kim, S., Kim, J., Lee, D. K., Park, W., Kim, T., Jung, J., Hwang, J. Y., Won, M. H., Ryoo, S., Kang, S. G., Ha, K. S., Kwon, Y. G. and Kim, Y. M. (2019) NF-κB-responsive miR-155 induces functional impairment of vascular smooth muscle cells by downregulating soluble guanylyl cyclase. *Exp. Mol. Med.* **51**, 17.

Park, U. C., Shin, J. Y., McCarthy, L. C., Kim, S. J., Park, J. H., Chung, H. and Yu, H. G. (2014) Pharmacogenetic associations with long-term response to anti-vascular endothelial growth factor treatment in neovascular AMD patients. *Mol. Vis.* **20**, 1680-1694.

Pierce, E. A., Avery, R. L., Foley, E. D., Aiello, L. P. and Smith, L. E. (1995) Vascular endothelial growth factor/vascular permeability factor expression in a mouse model of retinal neovascularization. *Proc. Natl.Acad. Sci. U.S.A.* **92**, 905-909.

Semeraro, F., Morescalchi, F., Duse, S., Parmeggiani, F., Gambicorti, E. and Costagliola, C. (2013) Aflibercept in wet AMD: specific role and optimal use. *Drug. Des. Devel. Ther.* **7**, 711-722.

Shah, R. S., Soetikno, B. T., Lajko, M. and Fawzi, A. A. (2015) A mouse model for laser-induced choroidal neovascularization. *J. Vis. Exp.* **106**, e53502.

Shibuya, M. (2006) Vascular endothelial growth factor receptor-1 (VEGFR-1/Flt1): a dual regulator for angiogenesis. *Angiogenesis* **9**, 225-230.

Shi, F., Wang, Y. C., Zhao, T. Z., Zhang, S., Du, T. Y., Yang, C. B., Li, Y. H. and Sun, X. Q. (2012) Effects of simulated microgravity on human umbilical vein endothelial cell angiogenesis and role of the PI3K-Akt-eNOS signal pathway. *PLoS ONE* **7**, e40365.

Simo, R. and Hernandez, C. (2008) Intravitreous anti-VEGF for diabetic retinopathy: hopes and fears for a new therapeutic strategy. *Diabetologia* **9**, 1574-1580.

Spaide, R. F., Laud, K., Fine, H. F., Klancnik, J. M., Jr., Meyerle, C. B., Yannuzzi, L. A., Sorenson, J., Slakter, J., Fisher, Y. L. and Coonet, M. J. (2006) Intravitreal bevacizumab treatment of choroidal neovascularization secondary to age-related macular degeneration. *Retina* **26**, 383-390.

Taimeh, Z., Loughran, J., Birks, E. J. and Bolli, R. (2013) Vascular endothelial growth factor in heart failure. *Nat. Rev. Cardiol.* **9**, 519-530.

Veloso, C. E., de, Almeida, L. N., Recchia, F. M., Pelayes, D. and Nehemy, M. B. (2014) VEGF gene polymorphism and response to intravitreal ranibizumab in neovascular age-related macular degeneration. *Ophthalmic. Res.* **51**, 1-8.

Yan, Z., Shi, H., Zhu, R., Li, L., Qin, B., Kang, L., Chen H. and Guan H. (2018) Inhibition of YAP ameliorates choroidal neovascularization via inhibiting endothelial cell proliferation. *Mol. Vis.* **24**, 83-93.